Amorphous/crystalline heterogeneous interface synergizing with in-situ generated dual Cl^-- repelling layers to realize ultrastable seawater oxidation

Aiiiao Guo, Qichen Chen, Ziwei Zhang, Ye Feng, Meichuan Liu[*, †]

School of Chemical Science and Engineering, Shanghai Key Lab of Chemical Assessment and Sustainability, Tongji University, 1239 Siping Road, Shanghai, 200092, China.

* Corresponding author.

Tel: +86 21-65988570;

Email: liumc@tongji.edu.cn (M. Liu).

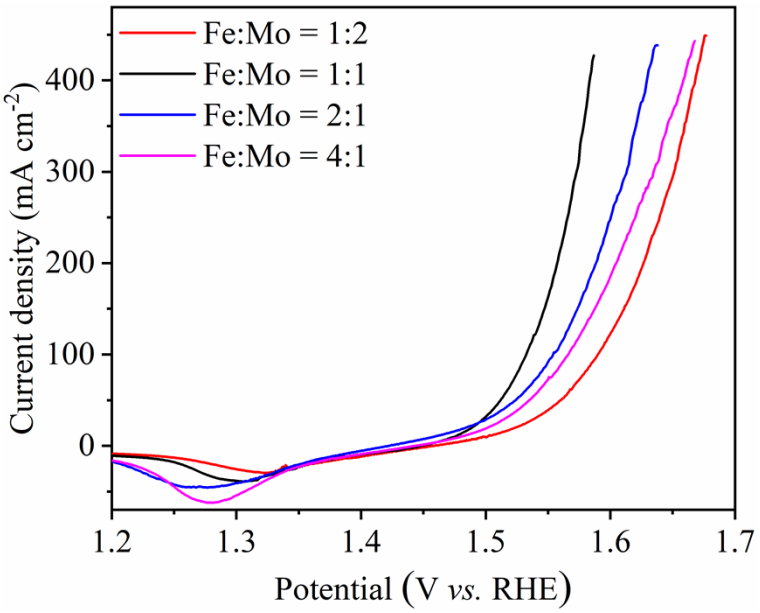

Fig. S1 The optimization of the ratio of the Fe:Mo.

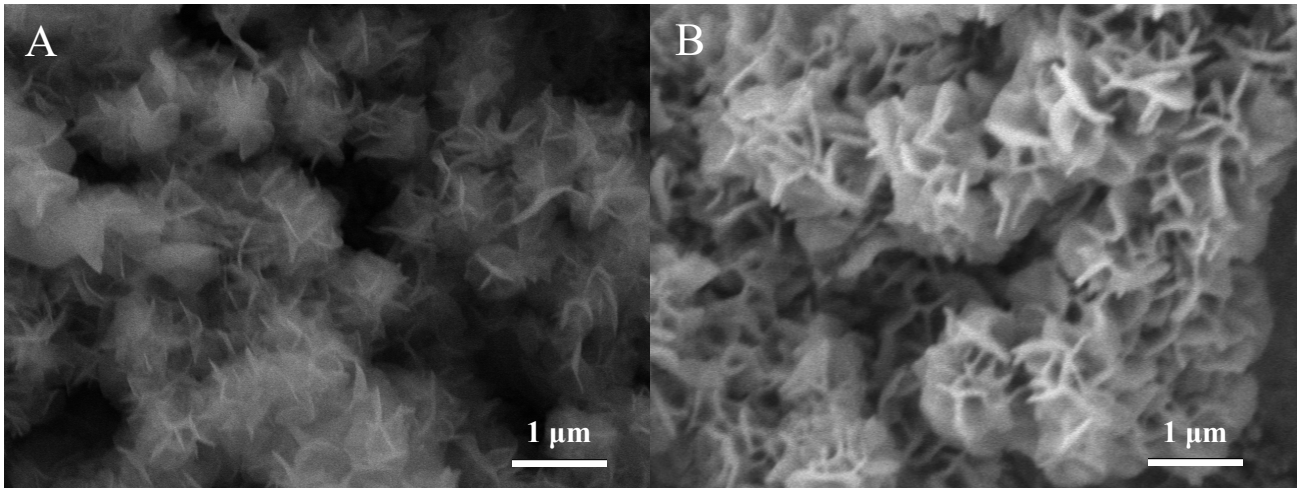

Fig. S2 The SEM image of $FeMoO_4/Ni_3S_2$(A) and FeMoP(B).

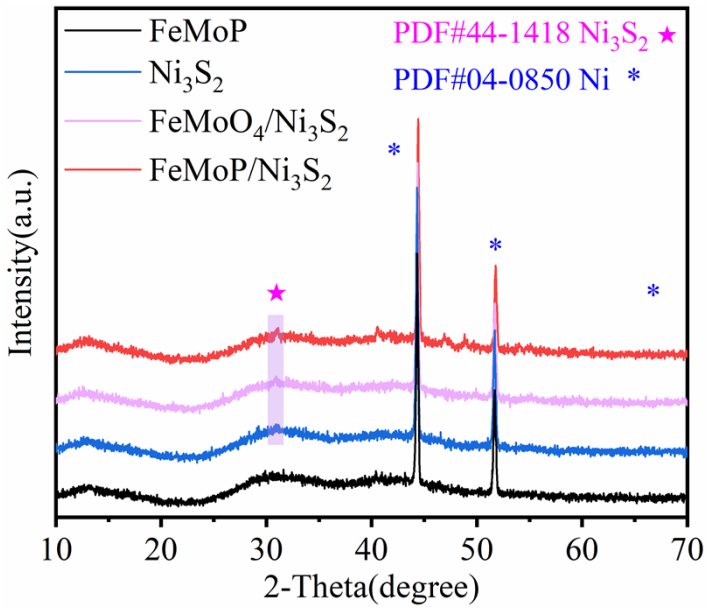

Fig. S3 XRD spectra for FeMoP, Ni_3S_2, $FeMoO_4/Ni_3S_2$ and $FeMoP/Ni_3S_2$.

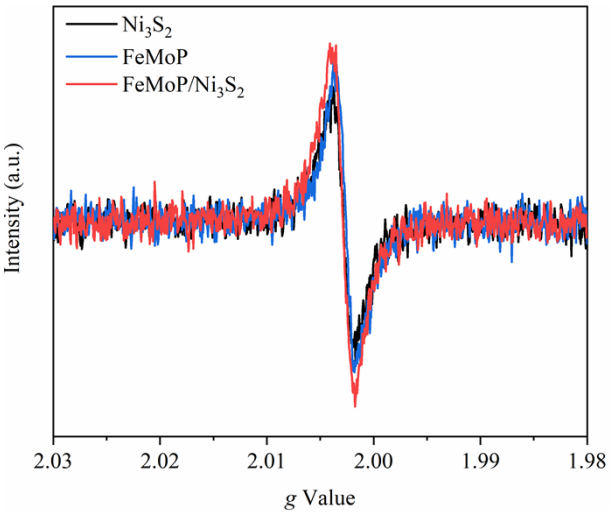

Fig. S4 ESR spectra for Ni_3S_2, FeMoP, and FeMoP/Ni_3S_2.

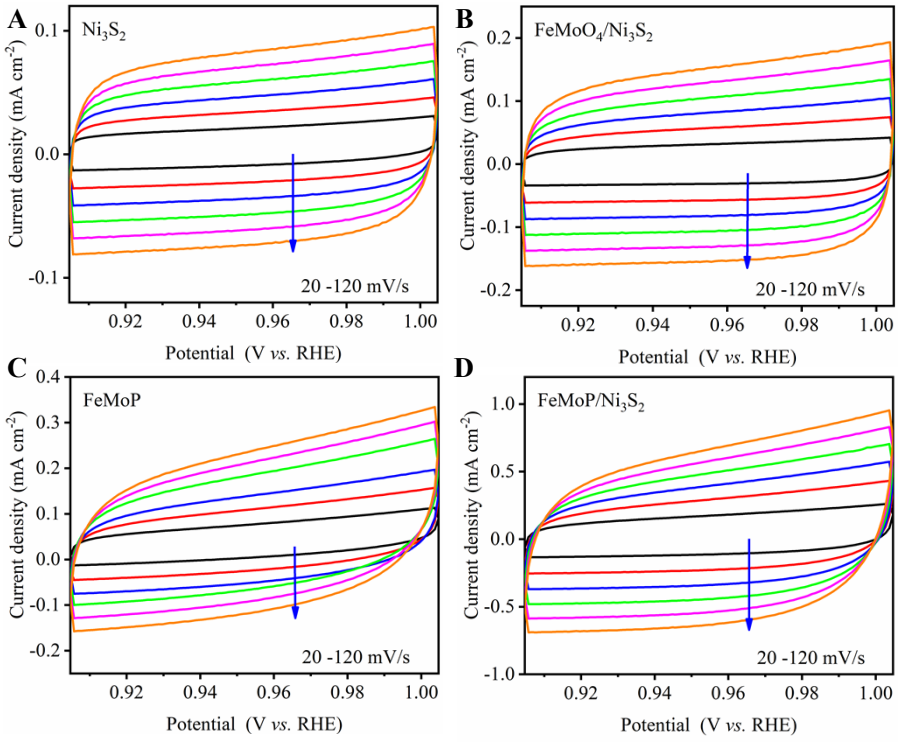

Fig. S5 CV curves of (A) Ni_3S_2; (B) $FeMoO_4/Ni_3S_2$; (C) FeMoP; (D) $FeMoP/Ni_3S_2$ at scan rates of 20 -120 mV s^{-1}.

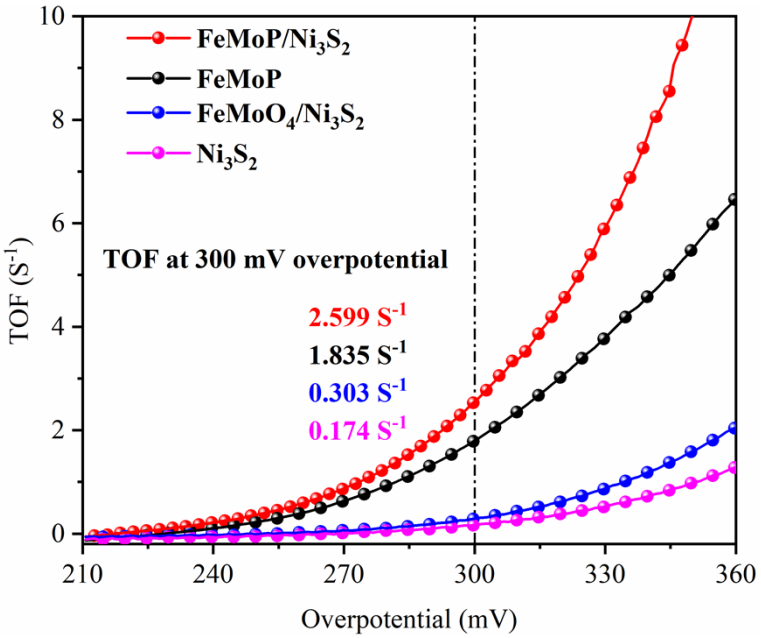

Fig. S6 The relationship between TOF and overpotential for $FeMoP/Ni_3S_2$, FeMoP, $FeMoO_4/Ni_3S_2$, and Ni_3S_2.

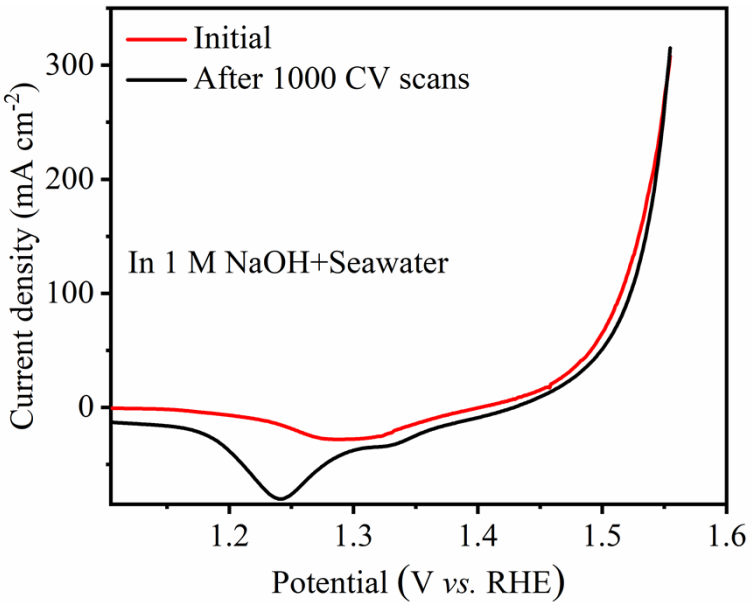

Fig. S7 LSV curves before and after 1000 CV scans in alkaline Seawater.

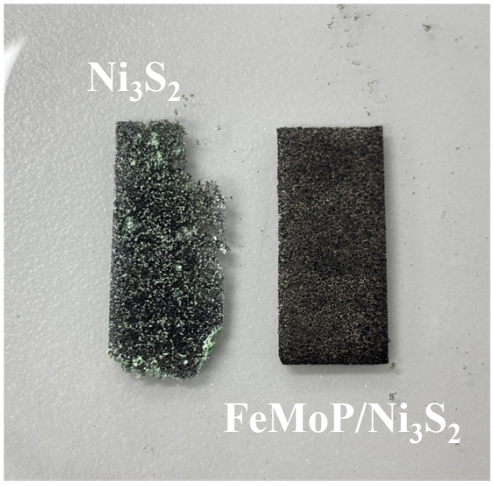

Fig. S8 Optical photos of different electrodes after 24 h electrolysis.

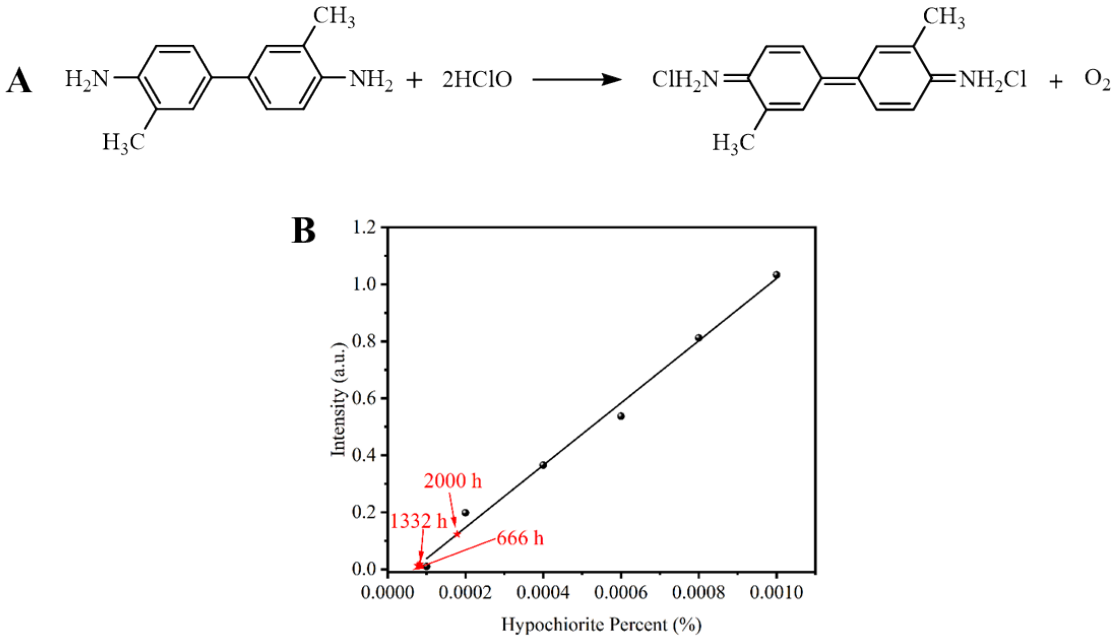

Fig. S9 (A) The chemical reaction between *o*-tolidine and HClO; (B) Calibration curve obtained by plotting the concentration of ClO^- against the corresponding absorption peak intensity at 436 nm. The R^2 of this curve is 0.99. The red stars mark the ClO^- absorbance in electrolyte after different OER running time.

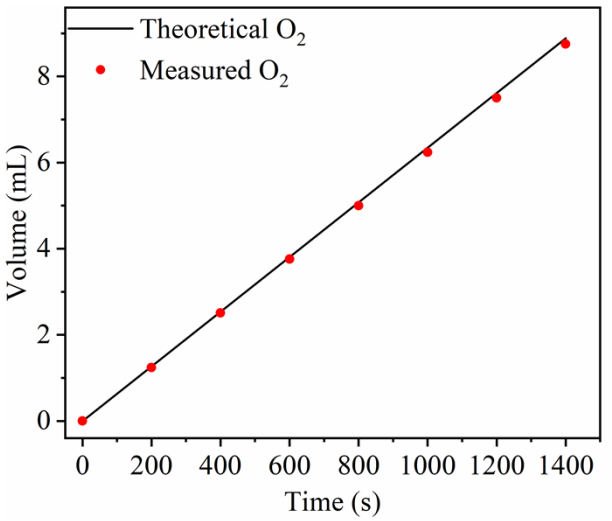

Fig. S10 Theoretical and experimental quantities of evolved gases in the 1500 s stability test.

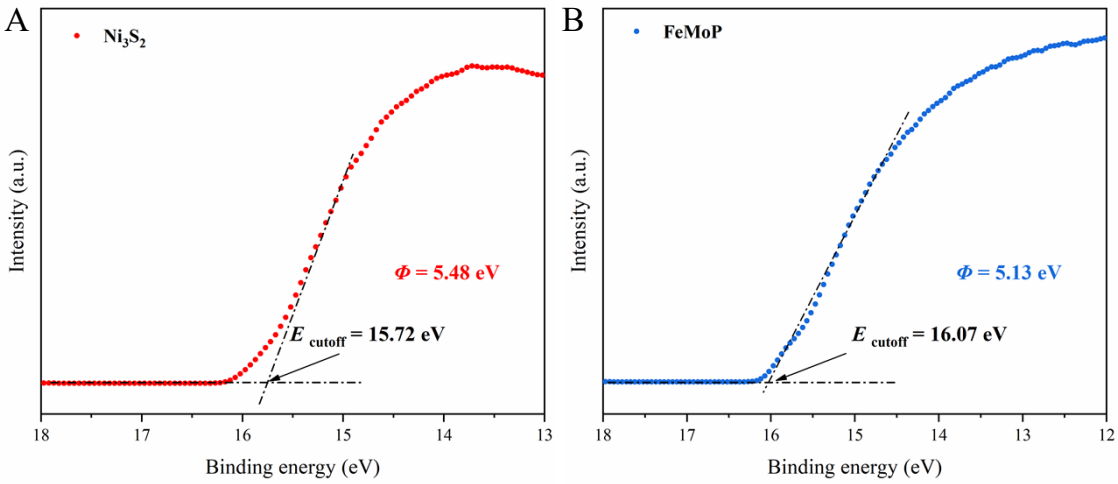

Fig. S11 UPS spectra in the cutoff energy region of Ni_3S_2 (A) and FeMoP (B).

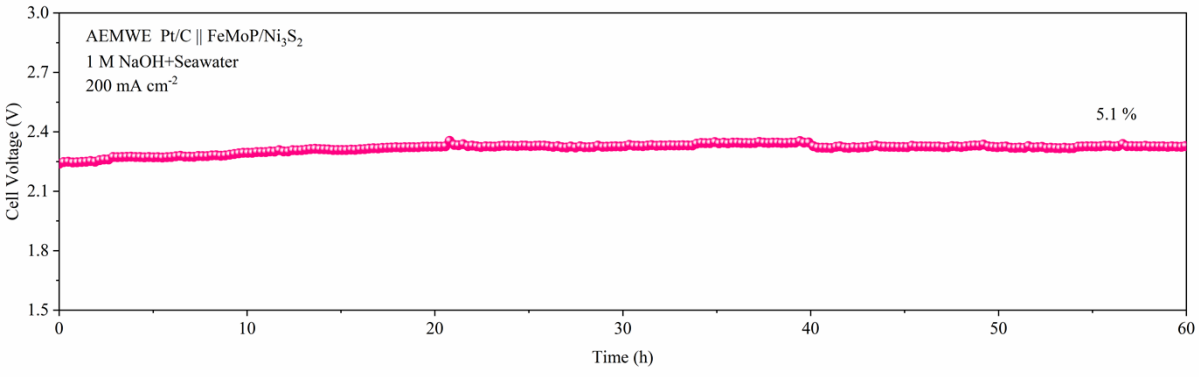

Fig. S12 The stability test at 200 mA cm^{-2} for Pt/C || $FeMoP/Ni_3S_2$ based AEMWE system in alkaline Seawater.

Table S1. Electrochemical parameters of different electrodes in alkaline seawater.

Sample	E_{corr} (V vs. RHE)	I_{corr} (A cm^{-2})
Ni_3S_2	-0.0733	3.480×10^{-4}
FeMoP	-0.0573	3.012×10^{-4}
Ni_3S_2/FeMoP	-0.0643	2.438×10^{-4}

Tabel S2. OER performance of different catalysts in 1.0 M NaOH/KOH

Catalysts	Substrate	Overpotential @ 100 (mV @ mA cm^{-2})	Reference
Mo-NiP	NF	339	Adv. Energy Mater. 2024, 2403009[1]
Ir-$Co_2P/Co_2P_2O_7$ NWs	NF	450	Appl. Catal. B Environ. 327 (2023) 122467[2]
B-$MnFe_2O_4$@MFOC	NF	334	Appl. Catal. B Environ. 330 (2023) 122577[3]
Mo-NiCo LDHs	CC	361	Chem. Eng. J, 2023, 463, 142396[4]
NiFeVP	NF	360	J. Mater. Chem. A, 2021, 9, 1220[5]
$CoNiPO_x$@V-Co_4N	NF	335	Adv. Sci., 2022,9, 2201311[6]
1D-Cu@Co-CoO/Rh	CF	380	Small, 2021, 17, 2103826[7]
P-CoVO	NF	372	Adv. Mater. 2024, 36, 2408634[8]
$FeMoP/Ni_3S_2$	NF	301	This work

Table S3. Ion concentrations in electrolyte after 24 h CP test at 200 mA cm^{-2}.

Catalysts	Ni concentration (ppm)	Fe concentration (ppm)
Ni_3S_2	103.0	/
FeMoP/Ni_3S_2	31.61	0.093

Tabel S3. OER performance of different catalysts in 1.0 M NaOH/KOH+Seawater

Catalysts	Substrate	Overpotential @ 100 (mV @ mA cm^{-2})	Reference
$NiFe/NiS_x$	NF	350	Proc. Natl Acad. Sci. USA 2019, 116, 6624–6629[9]
NiCoS	NF	360	Appl. Catal., B, 2021, 291, 120071[10]
NiIr LDH	NF	315	J. Am. Chem. Soc. 144 (2022) 9254-9263[11]
NiFe LDH@Co_3O_4	NF	358	Appl. Catal., B 317 (2022) 121799[12]
Mo-NiP	NF	390	Adv. Energy Mater. 2024, 2403009[1]
B-$MnFe_2O_4$@MFOC	NF	405	Appl. Catal. B Environ. 330 (2023) 122577[3]
NRAHM-NiO	NF	340	ACS Catal. 13(8) (2023) 5516-5528[13]
MoO_3@CoO	CC	404	Nat. Commun. 15(1) (2024) 2481[14]
Ni_xCr_yO	CP	370	Angew. Chem. Int. Ed. 62(40) (2023) e202309854[15]
FeMoP/Ni_3S_2	NF	308	This work

Reference:

[1] W. Hao, X. Ma, L. Wang, Y. Guo, Q. Bi, J. Fan, et al., *Adv. Energy Mater.* **2025**, 15, 202403009.

[2] V. H. Hoa, M. Austeria, H. T. Dao, M. Mai, D. H. Kim, *Appl. Catal., B* **2023**, 327, 122467.

[3] M. Chen, N. Kitiphatpiboon, C. Feng, Q. Zhao, A. Abudula, Y. Ma, et al., *Appl. Catal., B* **2023**, 330, 122577.

[4] K. Chen, Y.-H. Cao, S. Yadav, G.-C. Kim, Z. Han, W. Wang, et al., *Chem. Eng. J.* **2023**, 463, 142396.

[5] K. Sun, Y. Kou, H. Dong, S. Ye, D. Zhao, J. Liu, et al., *J. Mater. Chem. A* **2021**, 9, 1213.

[6] T. I. Singh, A. Maibam, D. C. Cha, S. Yoo, R. Babarao, S. U. Lee, et al., *Adv. Sci.* **2022**, 9, 202201311.

[7] T. Phan Khanh Linh, T. Duy Thanh, D. Malhotra, S. Prabhakaran, D. H. Kim, N. H. Kim, et al., *Small* **2021**, 17, 202103826.

[8] Z. Liang, D. Shen, Y. Wei, F. Sun, Y. Xie, L. Wang, et al., *Adv. Mater.* **2024**, 36, 202408634.

[9] Y. Kuang, M. J. Kenney, Y. Meng, W.-H. Hung, Y. Liu, J. E. Huang, et al., *Proc. Natl Acad. Sci. USA* **2019**, 116, 6624.

[10] C. Wang, M. Zhu, Z. Cao, P. Zhu, Y. Cao, X. Xu, et al., *Appl. Catal., B* **2021**, 291, 120071.

[11] H. You, D. Wu, D. Si, M. Cao, F. Sun, H. Zhang, et al., *J. Am. Chem. Soc.* **2022**, 144, 9254.

[12] C. Lyu, J. Cheng, K. Wu, J. Wu, N. Wang, Z. Guo, et al., *Appl. Catal., B* **2022**, 317, 121799.

[13] K. Hemmati, A. Kumar, A. R. Jadhav, O. Moradlou, A. Z. Moshfegh, H. Lee, *Acs Catal.* **2023**, 13, 5516.

[14] L. Zhou, D. Guo, L. Wu, Z. Guan, C. Zou, H. Jin, et al., *Nat. Commun.* **2024**, 15, 2481.

[15] D. Liu, Y. Cai, X. Wang, Y. Zhuo, X. Sui, H. Pan, et al., *Energy Environ. Sci.* **2024**, 20.